Journal of Molecular Structure 1223 (2020) 128995

Contents lists available at ScienceDirect

Journal of Molecular Structure

journal homepage: www.elsevier.com/locate/molstr

Novel derivatives of salicylanilide: Synthesis, characterization, PPO inhibitory activity and cytotoxicity

Hua Fang[a], Honghui Guo[a], Hui Chen[a], Jianyu Zhang[b], Zhuan Hong[a,*], Meijuan Fang[b,*]

[a] Third Institute of Oceanography, Ministry of Natural Resources, Technical Innovation Center for Utilization of Marine Biological Resources, Ministry of Natural Resources, Xiamen, 361005, China
[b] Fujian Provincial Key Laboratory of Innovative Drug Target Research and State Key Laboratory of Cellular Stress Biology, School of Pharmaceutical Sciences, Xiamen University, Xiamen 361102, China

ARTICLE INFO

Article history:
Received 11 June 2020
Revised 21 July 2020
Accepted 28 July 2020
Available online 29 July 2020

Keywords:
Synthesis
Salicylanilide analogues
Crystal
Ppo inhibitory
Cytotoxicity

ABSTRACT

Two series of novel salicylanilide analogues (**4a-4 g**) and (**4h-4t**) were designed, synthesized, and characterized, especially the structure of compound **4q** was further confirmed by single X-ray diffraction. The inhibitory activity on polyphenoloxidase (PPO) from the cephalothorax of Chinese white shrimp (*Fenneropenaeus chinensis*) was evaluated. The result indicated that all the synthesized derivatives (except **4 g** and **4t**) exhibited moderate PPO inhibitory properties having IC_{50} values in the range of 0.21 ± 0.19 to 4.32 ± 0.53 mM, whereas reference inhibitor salicylic acid and **3a** have IC_{50} values 3.93 ± 0.43 mM and 12.83 ± 0.51 mM, respectively. Specifically, 4-nitro-benzoic acid 3-(2–hydroxy–benzoylamino)- propyl ester (**4q**) exhibited the most potent PPO inhibitory activity with an IC_{50} value of 0.21 ± 0.19 mM. The kinetic studies of the compound (**4q**) demonstrated that the inhibitory effects of the compound on the PPO were belonging to competitive inhibitors. Meanwhile, the structure-activity relationship was discussed. Therefore, compound **4q** could act as a PPO inhibitor with anti-browning and antimicrobial properties to be applied in the food industry.

1. Introduction

Polyphenoloxidase (PPO) sometimes referred to as phenoloxidase, catecholase, phenolase, catechol oxidase, or even tyrosinase, is considered to be an *o*-diphenol. PPO (EC 1.14.18.1) is a multifunctional copper-containing enzyme that is widely distributed in microorganisms, plants, and animals [1–5]. PPO catalyzes both the hydroxylation of monophenols and the oxidation of diphenols into quinones, followed by non-enzymatic polymerization and autoxidation of quinones. It plays a crucial role in the formation of melanins or high molecular weight dark pigments [6,7]. Phenolic compounds have been investigated widely because of their potential pharmacological and biological properties. The free phenolic hydroxyl on the salicylic acid moiety is a functional group and is required for the activity that might function as proton shuttles that kill bacterial cells by destroying the cellular proton gradient [8]. 2-Hydroxy-*N*-phenylbenzamide, commonly known as salicylanilide, is a weakly acidic phenolic compound and has been highly noticed due to its significance in vitro antibacterial and antioxidant activities [9–11]. For example, salicylanilide benzoates [12], phenyl salicylanilide carbamates [13,14], dihalogenated salicylanilide carbamates [15] have antibacterial activities, acetylcholinesterase inhibitory activities, and antimycobacterial activities, respectively.

Nowadays, the inhibitory activity of salicylanilide analogues on PPO from cephalothoraxes of Chinese white shrimp is rarely reported. We herein synthesized a series of salicylanilide analogues by the reaction of salicylic acid propanolamine with the corresponding acyl chloride in Et_3N-contained solvents and evaluated their inhibitory activity on PPO isolated from cephalothoraxes of shrimp. Our ongoing research in this study includes the expansion of new salicylanilide derivatives and the evaluation of PPO-inhibitory activities. The designed salicylanilide compounds mainly focus on increasing their lipophilicity, which could decrease its cytotoxicity in cells and improve biological cell permeability [16]. Although lipophilicity seems to be one of the factors modulating positively the inhibition of PPO activity, an escalated lipophilicity could hamper in vitro evaluation due to solubility problems in testing media [17]. It hoped that these findings can lead to the discovery of potential preservative agents for the food industry and also offer key and useful information for the further design of highly potent PPO inhibitors. The structures of previously published salicylanilide carbamates in comparison with novel sal-

* Corresponding authors.
E-mail addresses: hfang@tio.org.cn (H. Fang), zhong@tio.org.cn (Z. Hong), fangmj@xmu.edu.cn (M. Fang).

https://doi.org/10.1016/j.molstruc.2020.128995
0022-2860/

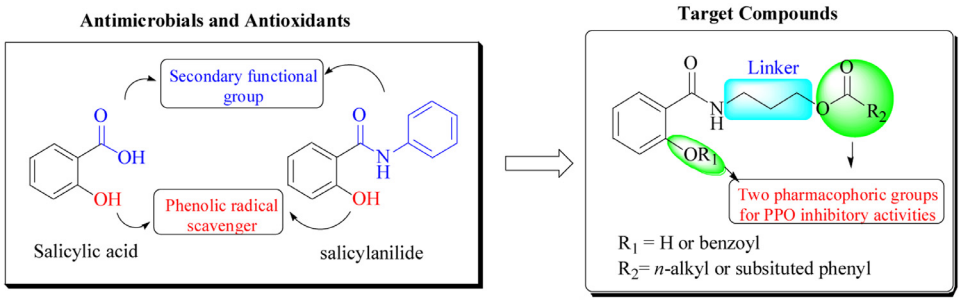

Fig. 1. Design of salicylic acid derivatives as PPO inhibitor.

icylanilide derivatives and the concept of design are depicted in Fig. 1.

2. Materials and methods

2.1. Chemicals and instruments

L-(3,4-dihydroxylphenyl)-alanine (L-DOPA), triethylamine (Et_3N), ammonium sulfate, methyl salicylate, 4-dimethylaminopyridine (DMAP), Brij 35 and 3-amino-1-propanol were purchased from Sigma-Aldrich (St. Louis, MO, USA). Other reagents used in this study were purchased from the domestic market and were all analytical purity used without further purification.

Melting points were determined on an SWG X-4 melting point apparatus and were uncorrected. Visible light absorption was tested on a UH5300 spectrophotometer (Hitachi, Japan). All NMR spectra were recorded on a Bruker 400 MHz NMR spectrometer, and DMSO–d6 was used as the solvent. High-resolution mass spectra (HRMS) data were acquired using a quadrupole-orbitrap (Q-Exactive) mass spectrometer (Thermo, UK) equipped with a heated electrospray ionization source (HESI-II). X-ray crystallographic data were collected on the Bruker X-ray diffractometer.

2.2. Synthesis of target compounds ***4a-4t***

The synthetic strategy of compounds **3a** and **4a-4t** were depicted in Scheme 1.

The procedure for the synthesis of 2–hydroxy–*N*-(3–hydroxy–alkyl)-benzamide **3a** was as follows: In a 100 mL round bottom flask, 3.04 g (0.02 mol) methyl salicylate and 3.00 g (0.04 mol) 3-amino-1-propanol were added [18]. The reaction mixture was stirred for 24 h at 80 °C, and the completion of the reaction was monitored by TLC. After completion of the reaction, the mixture was extracted with ethyl acetate and *tert*–pentyl alcohol (v/v = 1:1), the combined organic layer was dried over anhydrous $MgSO_4$ and concentrated in vacuo. The slurry residue was further purified by silica gel column chromatography (petroleum ether/ethyl acetate 1:5) to give 2–hydroxy–*N*-(3–hydroxy–propyl)-benzamide **3a** as colorless solid in a yield of 80%.

2-Hydroxy-*N*-(3–hydroxy–propyl)-benzamide (**3a**), m.p. 83.7–85.2 °C; ^{1}H NMR (400 MHz, DMSO–d_6): δ 12.84 (br, 1H, NH), 8.81 (s, 1H, OH), 7.83–7.80 (m, 1H, Ar), 7.37–7.35 (m, 1H, Ar), 6.89–6.84 (m, 2H, Ar), 4.02 (s, 1H, OH), 3.47–3.44 (m, 2H, OCH_2), 3.34–3.31 (m, 2H, $NHCH_2$), 1.72–1.66 (m, 2H, CH_2); ^{13}C NMR (100 MHz, DMSO–d_6): δ 169.4 (C = O), 160.6, 134.0, 128.0, 118.9, 117.8, 115.6 (Ar), 59.0 (OCH_2), 36.9 ($NHCH_2$), 32.5. HRMS (ESI, m/z): $[M + H]^+$ for $C_{10}H_{14}NO_3^+$, calculated 196.0968, found 196.0966.

The general procedure for the synthesis of target compounds **4a-4t** was as follows: In a 50 mL round bottom flask, 975 mg (5 mmol) of intermediate **3a**, DMAP (2 mmol, 244 mg) and 0.8 mL Et_3N were dissolved in 20 mL of dried CH_2Cl_2 solution in the ice bath, following by addition of the corresponding acyl chloride (2.4 mmol) [19]. The reaction was stirred overnight in the ice bath and concentrated in vacuo. The residue was purified by a silica gel column chromatography with petroleum ether/ethyl acetate (3:1, v/v) as eluent. Compounds **4a**-**4d** and **4r** are pale yellow oil. The solid product was then recrystallized from ethyl acetate to give **4e**-**4t** (except **4r**) as colorless crystal in yield of 59–88% (Scheme 1).

Acetic acid 3-(2–hydroxy–benzoylamino)-propyl ester (**4a**), pale yellow oil, yield: 77%; ^{1}H NMR (400 MHz, DMSO–d_6): δ 12.59 (s, 1H, NH), 8.84 (s, 1H, OH), 7.82–7.80 (m, 1H, Ar), 7.38–7.36 (m, 1H, Ar), 6.89–6.85 (m, 2H, Ar), 4.06–4.03 (m, 2H, OCH_2), 3.38–3.33 (m, 2H, $NHCH_2$), 1.98 (s, 3H, CH_3), 1.86–1.83 (m, 2H, CH_2), ^{13}C NMR (100 MHz, DMSO–d_6): δ 170.9, 169.5 (C = O), 160.6, 134.1, 128.0, 119.0, 117.8, 115.6 (Ar), 62.3 (OCH_2), 36.4 ($NHCH_2$), 28.5, 21.1. HRMS (ESI, m/z): $[M + H]^+$ for $C_{12}H_{16}NO_4^+$, calculated 238.1074, found 238.1069.

Butyric acid 3-(2–hydroxy–benzoylamino)-propyl ester (**4b**), pale yellow oil, yield: 66%; ^{1}H NMR (400 MHz, DMSO–d_6): δ 12.77 (s, 1H, NH), 9.00 (s, 1H, OH), 7.99–7.97 (m, 1H, Ar), 7.56–7.52 (m, 1H, Ar), 7.05–7.00 (m, 2H, Ar), 4.23–4.20 (m, 2H, OCH_2), 3.52–3.49 (m, 2H, $NHCH_2$), 2.41–2.32 (m, 2H, CH_2), 2.04–1.97 (m, 2H, CH_2), 1.72–1.62 (m, 2H, CH_2), 1.04–1.02 (m, 3H, CH_3); ^{13}C NMR (100 MHz, DMSO–d_6): δ 174.8, 169.6 (C = O), 160.6, 134.1, 128.0, 118.9, 117.8, 115.5 (Ar), 62.2 (OCH_2), 36.4 ($NHCH_2$), 36.0, 28.5, 18.4, 14.0. HRMS (ESI, m/z): $[M + H]^+$ for $C_{14}H_{20}NO_4^+$, calculated 266.1387, found 266.1381.

Hexanoic acid 3-(2–hydroxy–benzoylamino)-propyl ester (**4c**), pale yellow oil, yield: 59%, ^{1}H NMR (400 MHz, DMSO–d_6): δ 12.70 (s, 1H, NH), 8.47 (s, 1H, OH), 7.68–7.64 (m, 2H, Ar), 7.48–7.44 (m, 1H, Ar), 7.31–7.29 (m, 1H, Ar), 4.21–4.18 (m, 2H, OCH_2), 3.49–3.38 (m, 2H, $NHCH_2$), 2.67–2.63 (m, 2H, CH_2), 1.94–1.74 (m, 2H, CH_2), 1.48–1.40 (m, 6H, $3CH_2$), 1.05–0.99 (m, 3H, CH_3); ^{13}C NMR (100 MHz, DMSO–d_6): δ 173.4, 171.8 (C = O), 165.9, 148.2, 131.4, 130.2, 129.2, 123.6 (Ar), 62.1 (OCH_2), 36.3 ($NHCH_2$), 33.8, 31.1, 28.7, 24.6, 22.2, 14.2. HRMS (ESI, m/z): $[M + H]^+$ for $C_{16}H_{24}NO_4^+$, calculated 294.1700, found 294.1694.

Octanoic acid 3-(2–hydroxy–benzoylamino)-propyl ester (**4d**), pale yellow oil, yield: 87%, ^{1}H NMR (400 MHz, DMSO–d_6): δ 12.62 (s, 1H, NH), 8.84 (s, 1H, OH), 7.83–7.81 (m, 1H, Ar), 7.39–7.35 (m, 1H, Ar), 6.88–6.84 (m, 2H, Ar), 4.07–4.04 (m, 2H, OCH_2), 3.38–3.33 (m, 2H, $NHCH_2$), 2.28–2.22 (m, 2H, CH_2), 1.98–1.88 (m, 2H, CH_2), 1.50–1.46 (m, 2H, CH_2), 1.26–1.14 (m, 8H, $4CH_2$), 0.84–0.81 (m, 3H, CH_3); ^{13}C NMR (100 MHz, DMSO–d_6): δ 173.4, 169.6 (C = O), 160.6, 134.1, 128.0, 118.9, 117.8, 115.5 (Ar), 62.2 (OCH_2), 36.5 ($NHCH_2$), 33.9, 31.6, 28.9, 28.8, 28.5, 24.9, 22.5, 14.3. HRMS (ESI, m/z): $[M + H]^+$ for $C_{18}H_{28}NO_4^+$, calculated 322.2013, Found 322.2007.

Dodecanoic acid 3-(2–hydroxy–benzoylamino)-propyl ester (**4e**), white solid, m.p. 34.3–34.9, yield: 64%, ^{1}H NMR (400 MHz, DMSO–d_6): δ 12.78 (s, 1H, NH), 8.98 (s, 1H, OH), 7.98–7.96 (m, 1H, Ar), 7.55–7.51 (m, 1H, Ar), 7.04–7.00 (m, 2H, Ar), 4.23–4.19 (m, 2H, OCH_2), 3.52–3.49 (m, 2H, $NHCH_2$), 2.42–2.32 (m, 2H, CH_2), 2.03–1.98 (m, 2H, CH_2), 1.66–1.62 (m, 2H, CH_2), 1.38–1.32 (m, 16H,

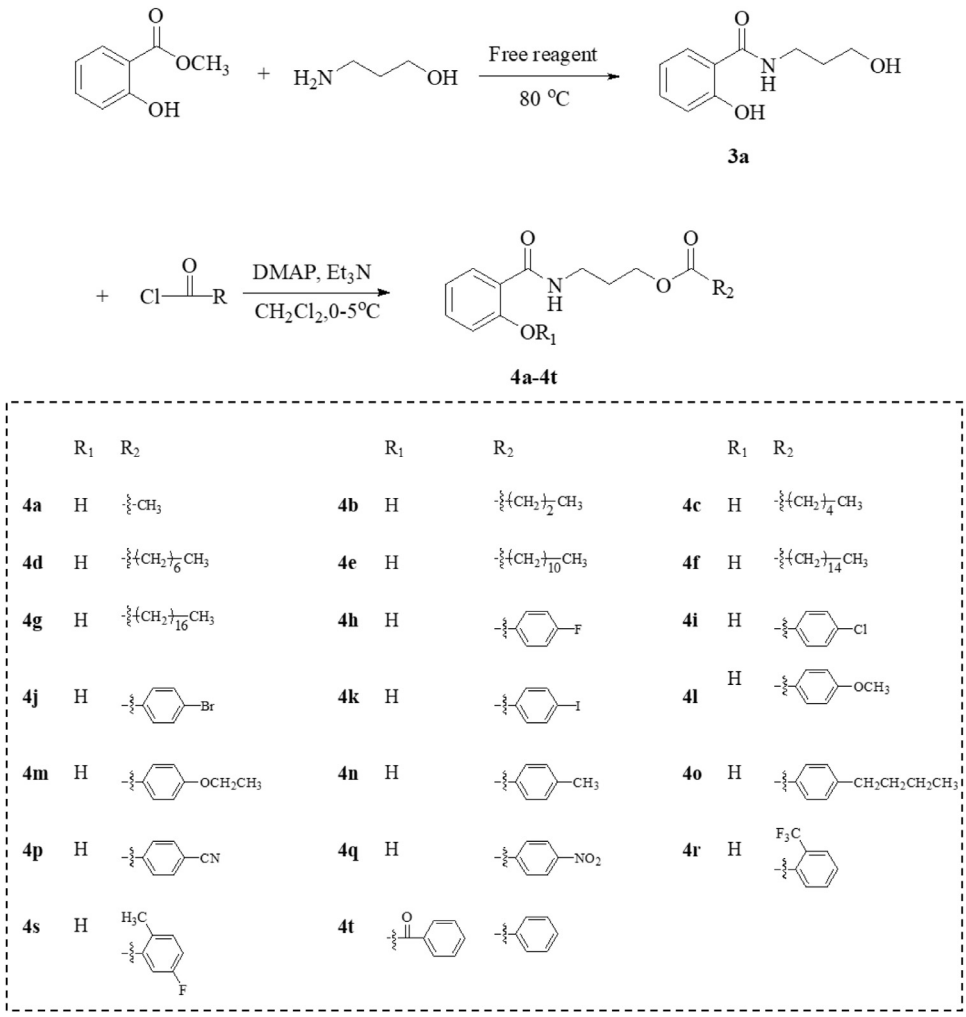

Scheme 1. General synthesis of compounds **4a**-**4t**.

8CH_2), 1.00–0.97 (m, 3H, CH_3); ^{13}C NMR (100 MHz, DMSO–d_6): δ 173.3, 169.6 ($C = O$), 160.7, 134.1, 128.0, 118.9, 117.8, 115.5 (Ar), 62.2 (OCH_2), 36.5 ($NHCH_2$), 33.9, 31.8, 29.4, 29.3, 29.3, 29.2, 29.1, 28.9, 28.5, 24.9, 22.5, 14.4. HRMS (ESI, *m/z*): $[M + H]^+$ for $C_{22}H_{36}NO_4^+$, calculated 378.2639, found 378.2649.

Hexadecanoic acid 3-(2–hydroxy–benzoylamino)-propyl ester (**4f**), white solid, m.p. 35.3–36.0, yield: 69%, ^{1}H NMR (400 MHz, DMSO–d_6): δ 12.78 (s, 1H, NH), 8.99 (s, 1H, OH), 7.98–7.96 (m, 1H, Ar), 7.55–7.51 (m, 1H, Ar), 7.04–7.00 (m, 2H, Ar), 4.23–4.20 (m, 2H, OCH_2), 3.53–3.48 (m, 2H, $NHCH_2$), 2.42–2.30 (m, 2H, CH_2), 2.03–1.97 (m, 2H, CH_2), 1.66–1.62 (m, 2H, CH_2), 1.42–1.37 (m, 24H, 12CH_2), 0.98–0.96 (m, 3H, CH_3); ^{13}C NMR (100 MHz, DMSO–d_6): δ 173.3, 169.6 ($C = O$), 160.7, 134.1, 128.0, 118.9, 117.8, 115.5 (Ar), 62.2 (OCH_2), 36.5 ($NHCH_2$), 33.9, 31.8, 29.5, 29.5, 29.5, 29.4, 29.4, 29.4, 29.3, 29.2, 29.1, 28.9, 28.5, 24.9, 22.6, 14.4. HRMS (ESI, *m/z*): $[M + H]^+$ for $C_{26}H_{44}NO_4^+$, calculated 434.3265, found 434.3258.

Octadecanoic acid 3-(2–hydroxy–benzoylamino)-propyl ester (**4 g**), white solid, m.p. 39.3–41.0, yield: 77%, ^{1}H NMR (400 MHz, DMSO–d_6): δ 12.78 (s, 1H, NH), 8.98 (s, 1H, OH), 7.98–7.96 (m, 1H, Ar), 7.55–7.51 (m, 1H, Ar), 7.04–7.00 (m, 2H, Ar), 4.23–4.20 (m, 2H, OCH_2), 3.53–3.48 (m, 2H, $NHCH_2$), 2.42–2.30 (m, 2H, CH_2), 2.03–1.97 (m, 2H, CH_2), 1.66–1.62 (m, 2H, CH_2), 1.38–1.34 (m, 28H, 14CH_2), 1.00–0.98 (m, 3H, CH_3); ^{13}C NMR (100 MHz, DMSO–d_6): δ 173.3, 169.6 ($C = O$), 160.7, 134.1, 128.0, 118.9, 117.8, 115.4 (Ar), 62.2 (OCH_2), 36.5 ($NHCH_2$), 33.9, 31.8, 29.5, 29.5, 29.5, 29.4, 29.4, 29.4, 29.3, 29.3, 29.3, 29.2, 29.1, 28.9, 28.5, 24.9, 22.6, 14.4. HRMS (ESI, *m/z*): $[M + H]^+$ for $C_{28}H_{48}NO_4^+$, calculated 462.3578, found 462.3570.

4-Fluoro-benzoic acid 3-(2–hydroxy–benzoylamino)-propyl ester (**4 h**), white solid, m.p. 63.1–64.3, yield: 72%, ^{1}H NMR (400 MHz, DMSO–d_6): δ 12.64 (s, 1H, NH), 8.93 (s, 1H, OH), 8.05–8.00 (m, 2H, Ar), 7.84–7.82 (m, 1H, Ar), 7.41–7.37 (m, 1H, Ar), 7.35–7.30 (m, 2H, Ar), 6.89–6.85 (m, 2H, Ar), 4.35–4.32 (m, 2H, OCH_2), 3.50–3.45 (m, 2H, $NHCH_2$), 2.05–1.98 (m, 2H, CH_2); ^{13}C NMR (100 MHz, DMSO–d_6): δ 169.6, 165.3 ($C = O$), 160.6, 134.1, 132.5, 132.4, 128.0, 126.9, 126.8, 118.9, 117.9, 116.4, 116.1, 115.6 (Ar), 63.3 (OCH_2), 36.6 ($NHCH_2$), 28.5. HRMS (ESI, *m/z*): $[M + H]^+$ for $C_{17}H_{17}FNO_4^+$, calculated 318.1136, found 318.1130.

4-Chloro-benzoic acid 3-(2–hydroxy–benzoylamino)-propyl ester (**4i**), white solid, m.p. 60.3–61.2, yield: 70%, ^{1}H NMR (400 MHz, DMSO–d_6): δ 12.62 (s, 1H, NH), 8.93 (s, 1H, OH), 7.97–7.94 (m, 2H, Ar), 7.84–7.81 (m, 1H, Ar), 7.58–7.55 (m, 2H, Ar), 7.42–7.37 (m, 1H, Ar), 6.90–6.85 (m, 2H, Ar), 4.36–4.33 (m, 2H, OCH_2), 3.50–3.46 (m, 2H, $NHCH_2$), 2.05–1.98 (m, 2H, CH_2); ^{13}C NMR (100 MHz, DMSO–d_6): δ 169.7, 165.4 ($C = O$), 160.6, 138.7, 134.1, 131.4, 129.3, 129.1, 128.0, 118.9, 117.9, 115.6 (Ar), 63.5 (OCH_2), 36.5 ($NHCH_2$), 28.5. HRMS (ESI, *m/z*): $[M + H]^+$ for $C_{17}H_{17}ClNO_4^+$, calculated 334.0841, found 334.0834.

4-Bromo-benzoic acid 3-(2–hydroxy–benzoylamino)-propyl ester (**4j**), white solid, m.p. 78.6–80.9, yield: 63%, ^{1}H NMR (400 MHz, DMSO–d_6): δ 12.61 (s, 1H, NH), 8.93 (s, 1H, OH), 7.89–7.81 (m, 3H, Ar), 7.72–7.70 (m, 2H, Ar), 7.42–7.38 (m, 1H, Ar), 6.90–6.85

(m, 2H, Ar), 4.36–4.33 (m, 2H, OCH_2), 3.50–3.45 (m, 2H, $NHCH_2$), 2.05–1.98 (m, 2H, CH_2); ^{13}C NMR (100 MHz, DMSO–d_6): δ 169.6, 165.5 ($C = O$), 160.6, 134.1, 132.3, 131.6, 129.4, 128.0, 127.8, 118.9, 117.9, 115.6 (Ar), 63.5 (OCH_2), 36.5 ($NHCH_2$), 28.5. HRMS (ESI, m/z): $[M + H]^+$ for $C_{17}H_{17}BrNO_4^+$, calculated 378.0335, found 378.0329.

4-Iodo-benzoic acid 3-(2–hydroxy–benzoylamino)-propyl ester (**4k**), white solid, m.p. 83.9–84.8, yield: 69%, ^1H NMR (400 MHz, DMSO–d_6): δ 12.61 (s, 1H, NH), 8.92 (s, 1H, OH), 7.90–7.88 (m, 2H, Ar), 7.83–7.81 (m, 1H, Ar), 7.71–7.69 (m, 2H, Ar), 7.42–7.38 (m, 1H, Ar), 6.90–6.85 (m, 2H, Ar), 4.35–4.32 (m, 2H, OCH_2), 3.50–3.45 (m, 2H, $NHCH_2$), 2.04–1.98 (m, 2H, CH_2); ^{13}C NMR (100 MHz, DMSO–d_6): δ 169.6, 165.9 ($C = O$), 160.6, 138.2, 134.1, 131.3, 129.7, 128.0, 119.0, 117.8, 115.6, 102.2 (Ar), 63.4 (OCH_2), 36.5 ($NHCH_2$), 28.5. HRMS (ESI, m/z): $[M + H]^+$ for $C_{17}H_{17}INO_4^+$, calculated 426.0197, found 426.0189.

4-Methoxy-benzoic acid 3-(2–hydroxy–benzoylamino)-propyl ester (**4l**), white solid, m.p. 71.6–72.3, yield: 71%, ^1H NMR (400 MHz, DMSO–d_6): δ 12.65 (s, 1H, NH), 8.94 (s, 1H, OH), 7.93–7.90 (m, 2H, Ar), 7.85–7.83 (m, 1H, Ar), 7.42–7.38 (m, 1H, Ar), 7.02–7.00 (m, 2H, Ar), 6.91–6.86 (m, 2H, Ar), 4.32–4.29 (m, 2H, OCH_2), 3.86 (s, 3H, OCH_3), 3.50–3.45 (m, 2H, $NHCH_2$), 2.03–1.98 (m, 2H, CH_2); ^{13}C NMR (100 MHz, DMSO–d_6): δ 169.6, 165.9 ($C = O$), 163.6, 160.7, 134.1, 131.7, 128.0, 122.5, 119.0, 117.9, 117.6, 114.4 (Ar), 62.8 (OCH_2), 56.0 (OCH_3), 36.6 ($NHCH_2$), 28.7. HRMS (ESI, m/z): $[M + H]^+$ for $C_{18}H_{20}NO_4^+$, calculated 330.1336, found 330.1331.

4-Ethoxy-benzoic acid 3-(2–hydroxy–benzoylamino)-propyl ester (**4 m**), white solid, m.p. 90.3–91.4, yield: 80%, ^1H NMR (400 MHz, DMSO–d_6): δ 12.65 (s, 1H, NH), 8.92 (s, 1H, OH), 7.91–7.89 (m, 2H, Ar), 7.85–7.83 (m, 1H, Ar), 7.42–7.38 (m, 1H, Ar), 7.00–6.98 (m, 2H, Ar), 6.91–6.86 (m, 2H, Ar), 4.31–4.28 (m, 2H, OCH_2), 4.12–4.07 (m, 2H, $NHCH_2$), 3.50–3.45 (m, 2H, OCH_2), 2.03–1.96 (m, 2H, CH_2), 1.36–1.33 (m, 3H, CH_3); ^{13}C NMR (100 MHz, DMSO–d_6): δ 169.6, 165.9 ($C = O$), 162.9, 160.7, 134.1, 131.7, 128.0, 122.3, 118.9, 117.9, 115.6, 114.8 (Ar), 64.0, 62.8 (OCH_2), 36.6 ($NHCH_2$), 28.7, 14.9. HRMS (ESI, m/z): $[M + H]^+$ for $C_{19}H_{22}NO_5^+$, calculated 344.1493, found 344.1485.

4-Methyl-benzoic acid 3-(2–hydroxy–benzoylamino)-propyl ester (**4n**), white solid, m.p. 60.0–61.5, yield: 65%, ^1H NMR (400 MHz, DMSO–d_6): δ 12.64 (s, 1H, NH), 8.92 (s, 1H, OH), 7.87–7.83 (m, 3H, Ar), 7.42–7.38 (m, 1H, Ar), 7.32–7.30 (m, 2H, Ar), 6.91–6.86 (m, 2H, Ar), 4.34–4.30 (m, 2H, OCH_2), 3.50–3.45 (m, 2H, $NHCH_2$), 2.38 (s, 3H, CH_3), 2.04–1.97 (m, 2H, CH_2); ^{13}C NMR (100 MHz, DMSO–d_6): δ 169.7, 166.2 ($C = O$), 144.0, 134.1, 129.7, 129.6, 128.0, 127.6, 119.0, 117.9, 117.6 (Ar), 63.0 (OCH_2), 36.6 ($NHCH_2$), 28.6, 21.6. HRMS (ESI, m/z): $[M + H]^+$ for $C_{18}H_{20}NO_5^+$, calculated 314.1387, found 314.1381.

4-Butyl-benzoic acid 3-(2–hydroxy–benzoylamino)-propyl ester (**4o**), white solid, m.p. 51.9–52.6, yield: 78%, ^1H NMR (400 MHz, DMSO–d_6): δ 12.64 (s, 1H, NH), 8.94 (s, 1H, OH), 7.88–7.82 (m, 3H, Ar), 7.42–7.38 (m, 1H, Ar), 7.32–7.29 (m, 2H, Ar), 6.90–6.86 (m, 2H, Ar), 4.34–4.31 (m, 2H, OCH_2), 3.50–3.45 (m, 2H, $NHCH_2$), 2.66–2.62 (m, 2H, CH_2), 2.04–1.97 (m, 2H, CH_2), 1.60–1.52 (m, 2H, CH_2), 1.32–1.26 (m, 2H, CH_2), 0.91–0.87 (m, 3H, CH_3); ^{13}C NMR (100 MHz, DMSO–d_6): δ 169.7, 166.2 ($C = O$), 160.7, 148.7, 134.1, 129.7, 129.0, 128.0, 127.8, 118.9, 117.9, 115.6 (Ar), 63.0 (OCH_2), 36.6 ($NHCH_2$), 35.2, 33.2, 28.6, 22.2, 14.2. HRMS (ESI, m/z): $[M + H]^+$ for $C_{21}H_{26}NO_4^+$, calculated 356.1856, found 356.1848.

4-Cyano-benzoic acid 3-(2–hydroxy–benzoylamino)-propyl ester (**4p**), white solid, m.p. 93.8–95.2, yield: 61%, ^1H NMR (400 MHz, DMSO–d_6): δ 12.60 (s, 1H, NH), 8.92 (s, 1H, OH), 8.11–8.08 (m, 2H, Ar), 7.99–7.97 (m, 2H, Ar), 7.82–7.80 (m, 1H, Ar), 7.41–7.37 (m, 1H, Ar), 6.91–6.85 (m, 2H, Ar), 4.39–4.36 (m, 2H, OCH_2), 3.51–3.46 (m, 2H, $NHCH_2$), 2.06–1.99 (m, 2H, CH_2); ^{13}C NMR (100 MHz, DMSO–d_6): δ 169.6, 165.0 ($C = O$), 160.6, 134.2, 134.1, 133.2, 130.2, 128.0, 119.0, 118.5, 117.9, 115.9 (Ar), 115.6 (CN), 63.9 (OCH_2), 36.5 ($NHCH_2$), 28.4. HRMS (ESI, m/z): $[M + H]^+$ for $C_{18}H_{17}N_2O_4^+$, calculated 325.1183, found 325.1177.

4-Nitro-benzoic acid 3-(2–hydroxy–benzoylamino)-propyl ester (**4q**), white solid, m.p. 123.0–125.1, yield: 78%, ^1H NMR (400 MHz, DMSO–d_6): δ 12.59 (s, 1H, NH), 8.92 (s, 1H, OH), 8.32–8.30 (m, 2H, Ar), 8.19–8.17 (m, 2H, Ar), 7.83–7.80 (m, 1H, Ar), 7.41–7.37 (m, 1H, Ar), 6.91–6.85 (m, 2H, Ar), 4.42–4.38 (m, 2H, OCH_2), 3.52–3.47 (m, 2H, $NHCH_2$), 2.08–1.99 (m, 2H, CH_2); ^{13}C NMR (100 MHz, DMSO–d_6): δ 169.6, 164.8 ($C = O$), 160.6, 150.7, 135.7, 134.1, 131.0, 128.0, 118.9, 117.8, 115.6 (Ar), 64.1 (OCH_2), 36.5 ($NHCH_2$), 28.4. HRMS (ESI, m/z): $[M + H]^+$ for $C_{17}H_{17}N_2O_6^+$, calculated 345.1081, found 345.1074.

2-Trifluoromethyl-benzoic acid 3-(2–hydroxy–benzoylamino)-propyl ester (**4r**), pale yellow oil, yield: 53%, ^1H NMR (400 MHz, DMSO–d_6): δ 12.59 (s, 1H, NH), 8.90 (s, 1H, OH), 7.89–7.77 (m, 5H, Ar), 7.42–7.38 (m, 1H, Ar), 6.91–6.86 (m, 2H, Ar), 4.38–4.34 (m, 2H, OCH_2), 3.47–3.42 (m, 2H, $NHCH_2$), 2.03–1.98 (m, 2H, CH_2); ^{13}C NMR (100 MHz, DMSO–d_6): δ 169.7, 166.6 ($C = O$), 160.6, 134.1, 133.3, 132.3, 130.5, 128.1, 127.2, 127.1, 119.0, 117.9 (Ar), 115.6 (CF_3), 64.2 (OCH_2), 36.3 ($NHCH_2$), 28.4. HRMS (ESI, m/z): $[M + H]^+$ for $C_{18}H_{17}F_3NO_4^+$, calculated 368.1104, found 368.1097.

5-Fluoro-2-methyl-benzoic acid 3-(2–hydroxy–benzoylamino)-propyl ester (**4 s**), white solid, m.p. 105.4–106.9, yield: 59%, ^1H NMR (400 MHz, $CDCl_3$): δ 10.71 (s, 1H, NH), 7.84–7.81 (s, 1H, OH), 7.50–7.46 (m, 1H, Ar), 7.21–7.18 (m, 1H, Ar), 7.10–7.01 (m, 3H, Ar), 6.99–6.85 (m, 1H, Ar), 6.15 (m, 1H, Ar), 4.53–4.50 (m, 2H, OCH_2), 3.63–3.60 (m, 2H, $NHCH_2$), 2.42 (s, 3H, CH_3), 2.17–2.11 (m, 2H, CH_2); ^{13}C NMR (100 MHz, DMSO–d_6): δ 170.3, 161.7 ($C = O$), 160.6, 136.0, 132.7, 132.6, 129.8, 119.3, 116.9, 113.8, 112.1 (Ar), 62.9 (OCH_2), 36.8 ($NHCH_2$), 28.9, 19.1. HRMS (ESI, m/z): $[M + H]^+$ for $C_{18}H_{19}FNO_4^+$, calculated 332.1293, found 332.1287.

Benzoic acid 3-[(2-*benzoyloxy*)-*benzoylamino*]-propyl ester (**4t**), white solid, m.p. 71.6–72.3, yield: 65%, ^1H NMR (400 MHz, DMSO–d_6): δ 8.50 (s, 1H, NH), 8.10–8.08 (m, 2H, Ar), 7.92–7.90 (m, 2H, Ar), 7.69–7.62 (m, 3H, Ar), 7.60–7.57 (m, 3H, Ar), 7.55–7.48 (m, 2H, Ar), 7.39–7.33 (m, 2H, Ar), 4.21–4.18 (m, 2H, OCH_2), 3.27–3.26 (m, 2H, $NHCH_2$), 1.98–1.80 (m, 2H, CH_2); ^{13}C NMR (100 MHz, DMSO–d_6): δ 166.1, 165.8, 164.8 ($C = O$), 148.3, 134.3, 133.7, 131.6, 130.4, 130.3, 129.6, 129.4, 129.3, 129.3, 129.1, 126.5, 123.7 (Ar), 62.8 (OCH_2), 36.2 ($NHCH_2$), 28.7. HRMS (ESI, m/z): $[M + H]^+$ for $C_{24}H_{22}NO_5^+$, calculated 404.1493, found 404.1485.

2.3. Preparation of PPO from the cephalothoraxes of chinese white shrimp

Chinese white shrimps with an average weight of 10.0 ± 0.5 g and an average body length of 10.5 ± 0.5 cm were purchased from the Xiashang supermarket in Xiamen, Fujian province, China. The cephalothoraxes of shrimps were immediately separated, pooled, and powdered by grinding with liquid nitrogen in a blender (DFT-200, China). All subsequent procedures for the extraction of PPO were conducted at 4 °C. Cephalothorax pulpy (150 g) was mixed with 450 mL of 0.05 M sodium phosphate buffer (pH 7.2) containing 1.0 M NaCl, and 0.2% Brij 35. The mixture was stirred continuously for 30 min, followed by centrifugation at 8000 g for 30 min using a refrigerated centrifuge (Hitachi, Japan). Solid ammonium sulfate (82.0 g) was added into the supernatant fraction to obtain 30% saturation. The precipitate was removed by centrifugation at 8000 g for 30 min using a refrigerated centrifuge (Hitachi, Japan). Another 43.0 g solid ammonium sulfate was added into the supernatant fraction to obtain 45% saturation. The precipitate was collected by centrifugation at 10,000 g for 30 min using a refrigerated centrifuge (Hitachi, Japan). The pellet obtained was dissolved in 5 mL 0.05 M sodium phosphate buffer, pH 7.2, and dialyzed against 1.0 L of the same buffer with three changes of dialysis buffer [20]. Finally, the insoluble materials were removed by centrifugation at

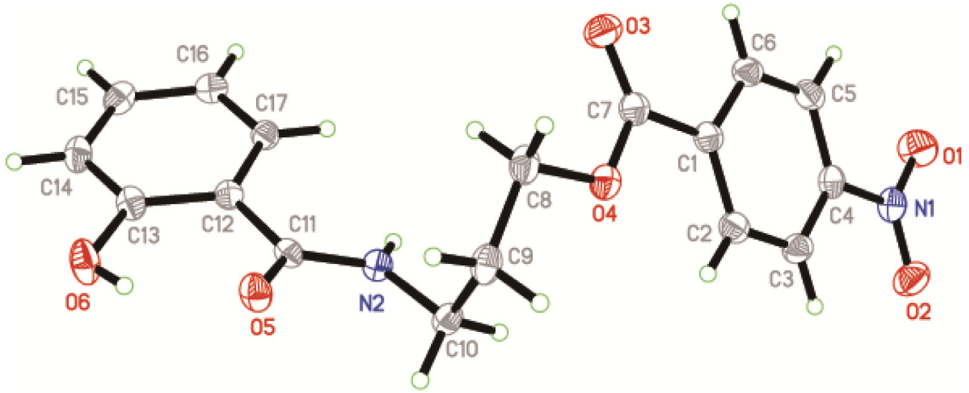

Fig. 2. ORTEP drawing of the molecular structure of **4q**. Displacement ellipsoids are at 50% probability level.

3000 g at 4 °C for 30 min and the supernatant was freeze-dried as "crude PPO" powder.

2.4. PPO activity assay

PPO activity was assayed using L-DOPA as a substrate according to the method of literature with a slight modification [21]. The assay system consisted of 10 μL of PPO solution (0.1 g/mL), 120 μL of 15 mM L-DOPA in deionized water, 100 μL of 0.05 M phosphate buffer (pH 6.0), and 10 μL of dimethyl sulfoxide (DMSO). The PPO activity was determined by monitoring the formation of dopachrome at 475 nm for 10 min at room temperature (25–28 °C) using a UH5300 spectrophotometer (Hitachi, Japan).

To study the inhibitory effect of salicylanilide analogues toward PPO, the crude PPO activity of 240.5 U/mg was incubated with salicylanilide analogues at a ratio of 1:1 (*v*/*v*) to obtain the suitable concentration. The assay system consisted of 10 μL of PPO solution (0.1 g/mL), 120 μL of 15 mM L-DOPA in deionized water, 100 μL of 0.05 M phosphate buffer (pH 6.0), and 10 μL the different concentrations of salicylanilide analogues dissolved in DMSO. The mixtures were allowed to stand for 5 min at room temperature before testing at 475 nm [22]. Enzyme and substrate blanks were prepared by excluding the substrate and enzyme, respectively. PPO inhibitory activity was determined and expressed as IC_{50}. PPO inhibitory activity was calculated as follows.

$$\text{PPOinhibition}\ (\%) = [(B - S)/B] \times 100$$

Where B and S are PPO activity of the control and PPO activity in the presence of salicylanilide analogues, respectively. Each sample was assayed in triplicate and at least six different concentrations. The data were expressed as mean ± SE of three experiments.

Table 1
Crystal data and ORTEP drawing of the molecular structure of compound **4q**.

CCDC number	1,908,936
Empirical formula	$C_{17}H_{16}N_2O_6$
Formula weight	344.10
Crystal size (mm)	0.15 × 0.09 × 0.11
Crystal system	Monoclinic
space group	P 21/n
Unit cell dimensions	
a (Å)	8.0553(1)
b (Å)	22.4930(5)
c (Å)	9.0626(2)
α°	90.0
β°	107.808(2)
γ°	90.0
Volume (Å^3)	1563.37(5)
D (g/cm^3)/ *Z*	1.463/4
μ/mm^{-1}/ *F*(000)	0.949/720
radiation	Cu Kα (λ = 1.54184)
2θ range for data collection/°	7.8612 to 141.3678
index ranges	$-9 \le h \le 9$, $-26 \le k \le 26$, $-11 \le l \le 11$
reflections collected	8773
independent reflections	2834
data/restraints/parameters	2834/0/227
goodness-of-fit on F^2	1.036
final R indexes [$I \ge 2s$ (I)]	R_1 = 0.0333, wR_2 = 0.0877
final R indexes [all data]	R_1 = 0.0382, wR_2 = 0.0905
largest diff. peak/hole/e Å^{-3}	0.21/−0.22

2.5. X-ray diffraction

A suitable crystal was selected and detected on Bruker X-ray diffractometer equipped with a graphite monochromator Mo Kα radiation (λ = 0.7013). The crystal was kept at 100 (2) K during data collection. Using Olex 2, the structure was solved with the ShelXT structure solution program using direct methods and refined with the ShelXL refinement package using least-squares minimization [23–25].

2.6. Cell viability assay

Four types test cells (including human embryonic kidney cell line AD293, human immortalized keratinocyte cell line HaCaT, human normal liver cell line LO_2 and human embryonic lung cell line MRC-5) were cultured in 96-well plates at a density of 5 × 10^3 cells per well in DMEM (LO_2 in RPMI-1640, others in DMEM), supplemented with 10% fetal calf serum, 100 U/mL penicillin, and 100 mg/mL streptomycin [26]. The cells were incubated at 37 °C in 5% CO_2-humidified air for overnight. Compound **4q** were dissolved in dimethyl sulfoxide (DMSO) and diluted with medium to the final concentrations. The cells were treated with different doses of compound **4q** for 48 h, and DMSO as vehicle control. The solution of MTT (5 mg/mL) dissolved in PBS solution was added to each well of 96-well plate (10% medium volume) and cultured for another 4 h at 37 °C. After treatment with DMSO (100 μL/well), the absorbance value was measured by using a microplate reader at 490 nm.

2.7. Statistical analyses

All measurements performed in triplicate and means and standard deviations were determined from independent trials. Differences between means were evaluated by one-way analysis of variance (ANOVA) and Tukey's test was used for pairwise comparisons. Differences were considered significant at $p < 0.05$. Data were analyzed to obtain the correlation coefficient by SPSS v.20 (SPSS Inc., Chicago, IL, USA).

3. Results and discussion

3.1. Chemistry

The target compounds fatty acid 3-(2–hydroxy–benzoylamino)-propyl ester (**4a-4 g**) and substituted-benzoic acid 3-(2–hydroxy–benzoylamino)-propyl ester (**4h-4t**) are depicted in Scheme 1. The intermediate material 2–hydroxy–*N*-(3–hydroxy–propyl)-benzamide (**3a**) was prepared according to the literature method with a slight modification [27]. Then, the intermediate (**3a**) reacted with corresponding fatty acid chloride acyl / substituted-benzoyl chloride by nucleophilic substitution reaction catalytic by DMAP in the presence of Et_3N to give novel compounds fatty acid 3-(2–hydroxy–benzoylamino)-propyl ester (**4a-4 g**) / substituted-benzoic acid 3-(2–hydroxy–benzoylamino)-propyl ester (**4h-4t**) with good yields. The structures of all synthesized compounds **4a-4t** were confirmed by ^1H NMR, ^{13}C NMR, and HRMS. Especially, the structure of compound **4q** was further confirmed by single X-ray diffraction.

3.2. Crystal structure of compound *4q*

Single crystals of $C_{17}H_{16}N_2O_6$ (**4q**) were grown from ethyl acetate. A suitable crystal was selected and mounted on an Ultima IV X-ray diffractometer (Rigaku, Japan). The crystal was kept at 100 (2) K during data collection. The structures were solved by direct methods yielding the positions of all non-hydrogen atoms, and refined with a full-matrix least-squares procedure based on F^2 using the Olex2 program system. The crystal data and the final refinement details of compound **4q** are given in Table 1. Fig. 2 shows a perspective view of compound **4q** with the atomic labeling system. The crystal structure is stabilized by weak intermolecular hydrogen bonds and the two phenyl rings make a dihedral angle of 52.5 (3) °C. Crystallographic data (excluding structure factors) for the struc-

Table 2
PPO inhibitory activities of the synthesized compounds **4a-4t**

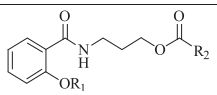

No	R_1	R_2	IC_{50} (±SE, mM)	No	R_1	R_2	IC_{50} (±SE, mM)
4a	H		4.32 ± 0.53	**4b**	H		3.27 ± 0.65
4c	H		0.64 ± 0.06	**4d**	H		0.31 ± 0.22
4e	H		0.35 ± 0.16	**4f**	H		1.78 ± 0.13
4g	H		**>5**	**4h**	H		1.25 ± 0.92
4i	H		0.86 ± 0.62	**4j**	H		0.68 ± 0.13
4k	H		0.26 ± 0.14	**4l**	H		0.52 ± 0.12
4m	H		0.42 ± 0.49	**4n**	H		0.52 ± 0.32
4o	H		0.28 ± 0.30	**4p**	H		0.72 ± 0.72
4q	H		0.21 ± 0.19	**4r**	H		0.79 ± 0.15
4s	H		0.54 ± 0.13	**4t**	COPh	Ph	>5
3a	/	/	12.83±0.51	SA	/	/	3.93 ± 0.43

[a] IC_{50} values: the concentration of the inhibitor required to produce 50% inhibition of PPO,

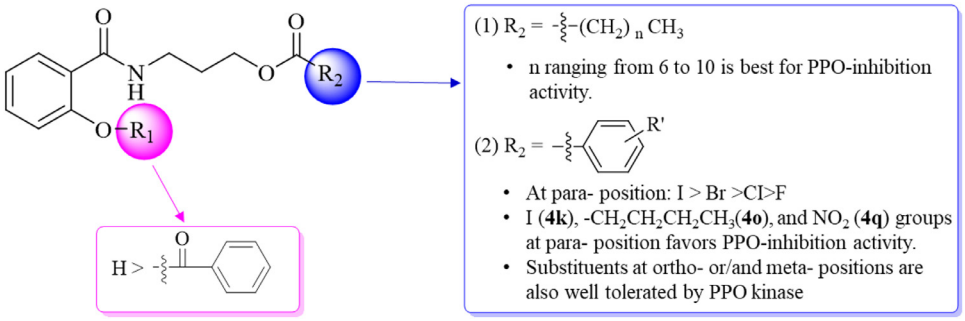

Fig. 3. Summarized SARs of synthesized compounds (**4a-4t**) in Scheme 1.

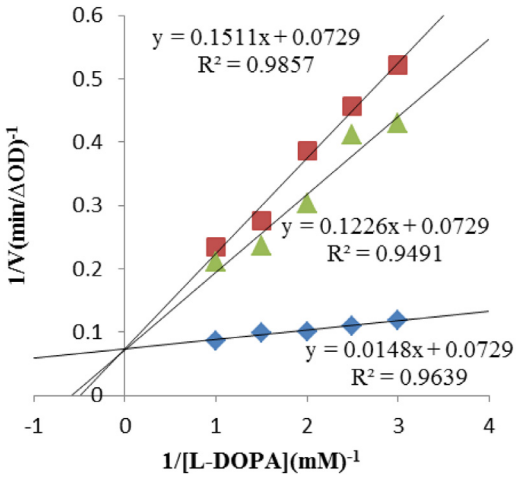

Fig. 4. Lineweaver-Burk plots for the inhibition of PPO from cephalothoraxes of Pacific white shrimp by compound **4q**. Concentrations of compound **4q** for curves were 0 mM (♦), 0.2 mM (▲), and 0.3 mM (■) respectively.

tures have been deposited in the Cambridge Crystallographic Data Center as supplementary publication No. CCDC 1,908,936.

3.3. PPO inhibition activity

The PPO inhibitory activity of synthetic salicylanilide analogues (**4a-4t**) was investigated by the usual procedure and compared with those of salicylic acid and intermediate **3a**. The IC_{50} value of all compounds tested is summarized in Table 2. The results in Table 2 indicated that most synthesized compounds (except **4 g** and **4t**) exhibited potent inhibitory effects on PPO with an IC_{50} value in the range of 0.21 ± 0.19 mM to 4.32 ± 0.53 mM, and they also displayed in vitro higher inhibitory activities on PPO than the reference inhibitor salicylic acid (SA) and intermediate material **3a**. The inhibitory activity of compound **4 g** was less than **3a,** which may be attributed to the fact that long fatty chains reduce the water solubility and are unfavorable to form interactions with enzyme PPO. On the other hand, benzoylation of the phenolic hydroxyl group (**4t**) resulted in a drastic reduction of activity, indicating that a free phenolic hydroxyl on the salicylic acid moiety is required for PPO inhibitory activity. Compounds **4d, 4e, 4k, 4o,** and **4q** had greater inhibitory activities than other synthesized compounds. In particular, compound **4q** exhibited the most potent PPO inhibitory activity with an IC_{50} value of 0.21 ± 0.19 mM.

From the inhibitory activities on PPO from cephalothoraxes of shrimp, preliminary structure-activity relationships (SAR) of target compounds (**4a**-**4**t) were carried out in this study (Fig. 3). Among compounds **4a-4 g** with aliphatic hydrocarbon substitution, when the number of carbon atoms in the *n*-alkyl group (R_2) was less than 8, the increase of the number of carbon atoms could increase activity. However, an *n*-alkyl group (R_2) having more than 11 carbon atoms was unfavorable for PPO inhibitory activity. For example, compound **4 g** carrying 17 carbon atoms in group R_2 was observed to sharply decline in the inhibitory activity of PPO. These results suggest that the substituent R_2 with different length of the carbon chain is important for the inhibition of PPO and *n*- aliphatic hydrocarbon substitution with n ranging from 6 to 10 was favorable for the improvement of the activity.

We then focused on exploring the SAR of compounds **4h-4t** which contained the aryl groups at the carbonyl position (R_2). In

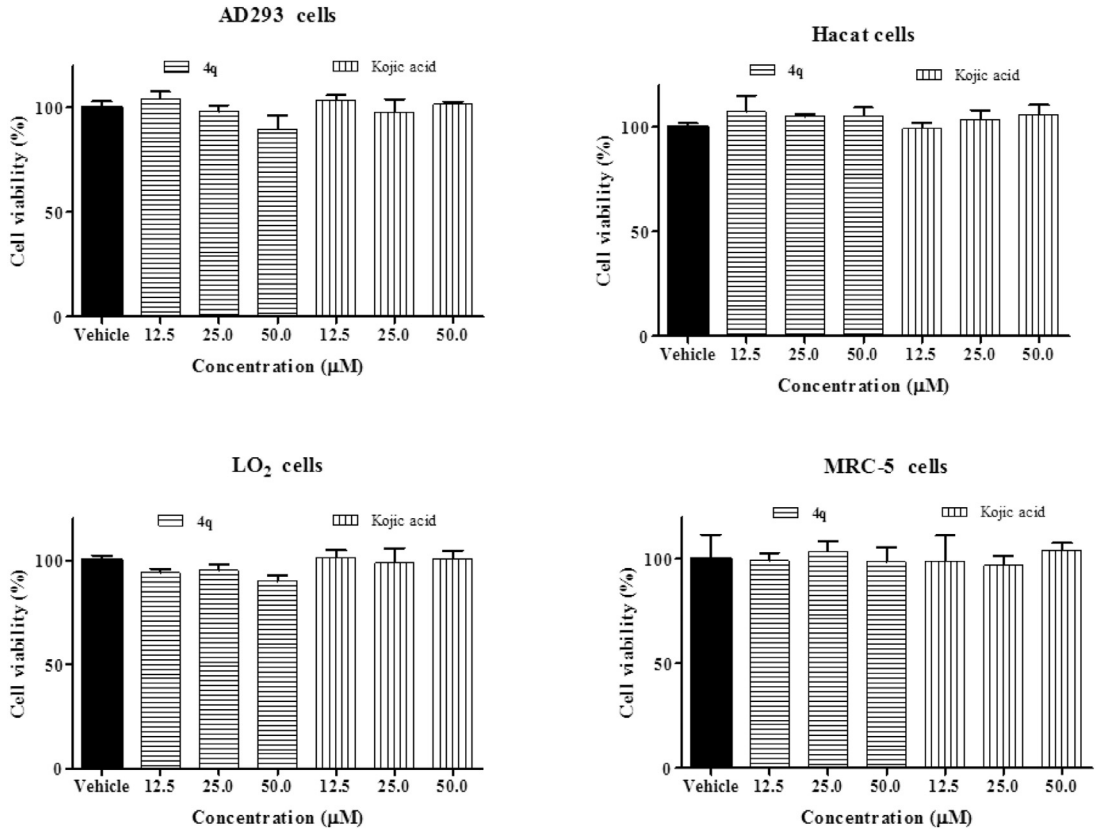

Fig. 5. Viability of AD293, Hacat, LO_2, and MRC-5 cells, treated with different concentrations of 12.5, 25.0, and 50.0 μM. Cytotoxic effects are expressed as percentage viabilities versus non-treated controls. No significance by Student's t-tests to control.

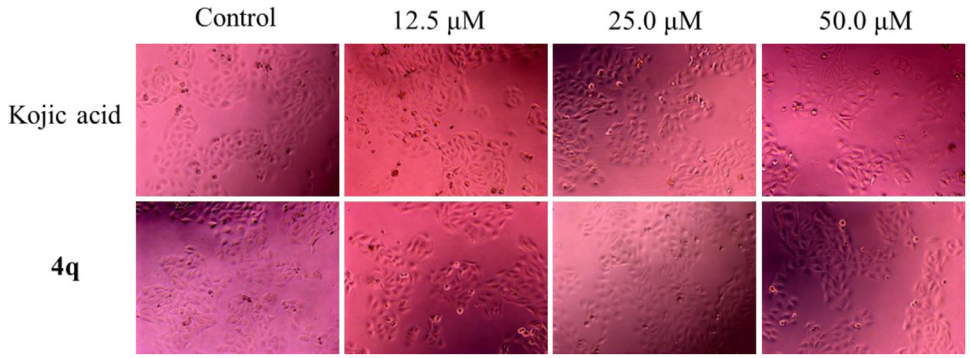

Fig. 6. Cytotoxic effects of kojic acid and compound **4q** in Hacat cells at concentrations of 12.5, 25.0, and 50.0 μM. .

compounds **4h**-**4t**, most compounds (except **4 h** and **4t**) exhibited potent PPO-inhibition activity, indicating that the introduction of an aromatic ring at R_2 position was also favorable on the PPO inhibitory. The effect of the substituent at the aromatic ring on PPO inhibition was investigated by introducing halogen, alkoxy, alkyl, and cyano groups. When the halogen substituents were introduced to the aromatic ring, we found that the inhibitory activities of these compounds (**4h**-**4k**) increased as the electronegativity of the halogen decreased ($F > Cl > Br > I$). On the other hand, **4 m** and **4o** showed better PPO inhibitory activity than **4l** and **4n**, indicating that the introduction of an *n*-alkyl or alkoxy groups with more than two carbon atoms at the C-4 position of the benzene ring was helpful for PPO inhibition activity. Finally, the introduction of cyano substituent into the benzene ring (**4p**) led to minor decrease activity and no significant increased PPO inhibitory activity could be observed for the compound with double substituted on the benzene ring (**4 s**). Taken together, compounds **4k, 4o**, and **4q** bearing the iodine, *n*–butyl, and nitro group at the 4-position of the phenyl group respectively, were found to be the most potent PPO-inhibition agents.

3.4. Inhibitory mechanism

Among all tested target compounds, **4q** showed the highest inhibitory activity, and we hence carried out the inhibition kinetic studies of **4q** towards PPO by using L-DOPA as a substrate. The Lineweaver-Burk plots for the inhibition of PPO by **4q** were obtained with variable concentrations of **4q** and the substrate (Fig. 4). The result of compound **4q** displayed that the 1/V vs. 1/[S] plot gave three straight lines with different slopes but with one intersection on the vertical axis, which indicated that **4q** acted as a competitive inhibitor of PPO. These results suggested that 4-nitro-benzoic acid 3-(2–hydroxy–benzoylamino)-propyl ester and its analogues could enter into the active center of enzyme PPO and bind to the active site of enzyme PPO to form the interactions with the free enzyme PPO. The *N*-nitro and hydroxy groups of salicylanilide analogues were essential for the PPO inhibitory activity, probably due to the copper chelating ability [28–29]. Therefore, we speculated that these series of synthesized compounds could serve as PPO competitive inhibitors to inhibit melanin formation in cephalothoraxes of shrimp.

3.5. Cytotoxicity screening of compound *4q*

To assess the safety of compound **4q**, it was tested for its toxicity in the human normal cell lines, including human embryonic kidney cell line AD293, human immortalized keratinocyte cell line HaCaT, human normal liver cell line LO_2 and human embryonic lung cell line MRC-5, by MTT at concentrations of 50.0 μM, 25.0 μM and 12.5 μM. When cells were incubated with 50 μg/mL **4q**, the cell viability was found to be higher than 90% for the four test human normal cell lines (Fig. 5). This concentration had no considerable cytotoxic effects on cell morphology and cell viability (Fig. 6).

In summary, we had synthesized two series of novel salicylanilides analogues including fatty acid 3-(2–hydroxy–benzoylamino)-propyl ester (**4a-4 g**) and substituted-benzoic acid 3-(2–hydroxy–benzoylamino)-propyl ester (**4h-4t**) as PPO inhibitors. The present study showed that most of the target compounds exhibited moderate PPO inhibitory activities with IC_{50} values in the range of 0.21 ± 0.19 to 4.32 ± 0.53 mM. Preliminary acute toxicity assay demonstrated that salicylanilides analogues were as safe as PPO inhibitors. All these data suggested that these molecules might be served as candidates for further development of preservation for cephalothoraxes of pacific white shrimp.

Credit author statement

Hua Fang: performed the synthesis experiment and designed the study. Honghui Guo: performed the synthesis experiment. Hui Chen: collected the crystal data. Jianyu Zhang: collected the SDS-page data and screened the cytotoxicity of compound. Zhuan Hong: reviewed and edited the manuscript. Meijuan Fang: conceived and designed the study.

Declaration of Competing Interest

The authors declare that they have no known competing financial interests or personal relationships that could have appeared to influence the work reported in this paper.

Acknowledgments

We appreciate the financial support from Marine Economy Innovation Development Area Demonstration Project of Beihai (Bhsfs003, Bhsfs009), and the Fundamental Research Funds for the Central Universities (No. 20720180051).

References

[1] M. Okot-Kotber, A. Liavoga, K.J. Yong, K. Bagorogoza, Activation of polyphenol oxidase in extracts of bran from several wheat (*Triticum aestivum*) cultivars using organic solvents, detergents, and chaotropes, J. Agr. Food Chem. 50 (2002) 2410–2417.
[2] F. Tinello, A. Lante, Recent advances in controlling polyphenol oxidase activity of fruit and vegetable products, Innov. Food Sci. Emerg. 50 (2018) 73–83.
[3] F. Solano, On the metal cofactor in the tyrosinase family, Int. J. Mol. Sci. 19 (2018) 633.
[4] K. Manheem, S. Benjakul, K. Kijroongrojana, W. Visessanguan, The effect of heating conditions on polyphenol oxidase, proteases and melanosis in pre–cooked Pacific white shrimp during refrigerated storage, Food Chem. 131 (2011) 1370–1375.

[5] S. Basiri, S.S. Shekarforoush, M. Aminlari, S. Akbari, The effect of pomegranate peel extract (PPE) on the polyphenol oxidase (PPO) and quality of Pacific white shrimp (*Litopenaeus vannamei*) during refrigerated storage, LWT-Food Sci. Technol. 60 (2015) 1025–1033.
[6] S. Ullan, C. Park, M. Ikram, D. Kang, S. Lee, J. Yang, Y. Park, S. Yoon, P. Chun, H.R. Moon, Tyrosinase inhibition and anti-melanin generation effect of cinnamamide analogues, Bioorg. Chem. 87 (2019) 43–55.
[7] P. Fronk, N. Jaeckels N, Influence of buffer systems on PPO activity of Riesling grapes [*Vitis vinifera subsp. vinifera cv. Riesling*], Eur. Food Res. Technol. 243 (2017) 859–865.
[8] I.Y. Lee, T.D. Gruber, A. Samuels, M. Yun, B. Nam, M. Kang, K. Crowley, B. Winterroth, H.I. Boshoff, C.E. Barry, Structure-activity relationships of antitubercular salicylanilides consistent with disruption of the proton gradient via proton shuttling, Bioorg. Med. Chem. 21 (2013) 114–126.
[9] J.A. Marrugal-Lorenzo, A. Serna-Gallego, J. Berastegui-Cabrera, J. Pachon, J. Sanchez-Cespedes, Repositioning salicylanilide anthelmintic drugs to treat adenovirus infections, Sci. Rep. 9 (2019) 17.
[10] Z.H. Guo, Y. Yin, C. Wang, P.F. Wang, X.T. Zhang, Z.C. Wang, H.L. Zhu, Design, synthesis and molecular docking of salicylic acid derivatives containing metronidazole as a new class of antimicrobial agents, Bioorg. Med. Chem. 23 (2015) 6148–6156.
[11] M. Kratky, M. Dzurkova, J. Janousek, K. Konecna, F. Trejtnar, J. Stolarikova, J. Vinsova, Sulfadiazine salicylaldehyde-based Schiff bases: synthesis, antimicrobial activity and cytotoxicity, Molecules 22 (2017) 1573.
[12] P. Skorna, M. Michalik, V. Luke, E. Klein, The structural analysis and modelling of ring substituent effect for the ortho-derivatives of 1-hydroxynaphthalene-2-carboxanilides and 2-hydroxynaphthalene-1-carboxanilides, J. Mol. Struct. 1144 (2017) 473–481.
[13] M. Kratky, J. Vinsova, Salicylanilide N-monosubstituted carbamates: synthesis and in vitro antimicrobial activity, Bioorg. Med. Chem. 24 (2016) 1322–1330.
[14] L. Zhang, L. Hou, W.Y. Sun, Z.D. Yu, J.B. Wang, H. Gao, G.M. Yang, Synthesis of p-O-alkyl salicylanilide derivatives as novel EGFR inhibitors, Drug Develop. Res. 77 (2016) 37–42.
[15] G. Paraskevopoulos, S. Monteiro, R. Vosatka, M. Kratky, L. Navratilova, F. Trejtnar, J. Stolarikova, J. Vinsova, Novel salicylanilides from 4,5-dihalogenated salicylic acids: synthesis, antimicrobial activity and cytotoxicity, Bioorg. Med. Chem. 25 (2017) 2530 -2530.
[16] S.S. Kumar, S. Athimoolam, B. Sridhar, Structural, spectral, theoretical and anticancer studies on new co-crystal of the drug 5-fluorouracil, J. Mol. Struct. 1173 (2018) 951–958.
[17] M.R. Naylor, A.M. Ly, M.J. Handford, et al., Lipophilic Permeability Efficiency Reconciles the Opposing Roles of Lipophilicity in Membrane Permeability and Aqueous Solubility, J. Med. Chem. 61 (2018) 11169–11182.
[18] I.M.C. Ienascu, M.A. Padure, A.X. Lupea, I. Balcu, I.M. Popescu, Synthesis and Characterization of Some New Salicylamide Derivatives with Potential Biological Activity, Rev. Chim-Bucharest 61 (2010) 368–371.
[19] Z. Baranyai, M. Kratky, R. Vosatka, E. Szabo, Z. Senoner, S. David, J. Stolarikova, J. Vinsova, S. Bosze, In vitro biological evaluation of new antimycobacterial salicylanilide-tuftsin conjugates, Eur. J. Med. Chem. 133 (2017) 152–173.
[20] N.P. Nirmal, S. Benjakul, Effect of ferulic acid on inhibition of polyphenoloxidase and quality changes of Pacific white shrimp (*Litopenaeus vannamei*) during iced storage, Food Chem. 116 (2009) 323–331.
[21] G. Karakaya, A. Ture, A. Ercan, S. Oncul, M.D. Aytemir, Synthesis, computational molecular docking analysis and effectiveness on tyrosinase inhibition of kojic acid derivatives, Bioorg. Chem. 88 (2019) 102950.
[22] G.H. Hui, W. Liu, H.L. Feng, J. Li, Y.Y. Gao, Effects of chitosan combined with nisin treatment on storage quality of large yellow croaker (*Pseudosciaena crocea*), Food Chem. 203 (2016) 276–282.
[23] O.V. Dolomanov, L.J. Bourhis, R.J. Gildea, J.A.K. Howard, H. Puschmann, a complete structure solution, refinement, and analysis program, J. Appl. Crystallogr. 42 (2009) 339–341.
[24] G.M. Sheldrick, Crystal structure refinement with SHELXL, Acta Crystallogr. C. 71 (2015) 3–8.
[25] G.M. Sheldrick, SHELXT-Integrated space-group and crystal structure determination, Acta Crystallogr. A 71 (2015) 3–8.
[26] T. Dincer, A.B.B. Er, ABB I. Er, I.B. Toraman, G. Yildiz, E. Kalay, RIPK4 suppresses the TGF-beta 1 signaling pathway in HaCaT cells, Cell Biolog. Inter. 44 (2020) 848–860.
[27] A. Manral, V. Saini, P. Meena, M. Tiwari, Multifunctional novel diallyl disulfide (DADS) derivatives with α-amyloid-reducing, cholinergic, antioxidant and metal chelating properties for the treatment of Alzheimer's disease, Bioorg. Med. Chem. 23 (2015) 6389–6403.
[28] S. Dogan, M.E. Diken, Y. Turhan, U. Alan, M. Dogan, M. Alkan, Characterization and inhibition of *Rosmarinus officinalis L.* polyphenoloxidase, Eur. Food Res. Technol. 233 (2011) 293–301.
[29] T. Sae-Leaw, S. Benjakul, Prevention of quality loss and melanosis of Pacific white shrimp by cashew leaf extracts, Food Control 95 (2019) 257–266.